



HAL
open science

Sound Scattering on a Turbulent, Weakly Heated Jet

A. Petrossian, J.-F. Pinton

► **To cite this version:**

A. Petrossian, J.-F. Pinton. Sound Scattering on a Turbulent, Weakly Heated Jet. *Journal de Physique II*, 1997, 7 (5), pp.801-812. 10.1051/jp2:1997152 . jpa-00248479

HAL Id: jpa-00248479

<https://hal.science/jpa-00248479v1>

Submitted on 4 Feb 2008

HAL is a multi-disciplinary open access archive for the deposit and dissemination of scientific research documents, whether they are published or not. The documents may come from teaching and research institutions in France or abroad, or from public or private research centers.

L'archive ouverte pluridisciplinaire **HAL**, est destinée au dépôt et à la diffusion de documents scientifiques de niveau recherche, publiés ou non, émanant des établissements d'enseignement et de recherche français ou étrangers, des laboratoires publics ou privés.

Sound Scattering on a Turbulent, Weakly Heated Jet

A. Petrossian ^(1,2) and J.-F. Pinton ^(1,*)

⁽¹⁾ Laboratoire de Physique, École Normale Supérieure de Lyon (**), 69364 Lyon France

⁽²⁾ Physics Department, Yerevan State University, 1 Manoukian street,
375049 Yerevan, Armenia

(Received 28 October 1996, revised 22 January 1997, accepted 13 February 1997)

PACS.42.68.-w – Atmospheric optics

PACS.43. – Acoustics

PACS.47.27.-i – Turbulent flows, convection, and heat transfer

Abstract. — We report an experimental study of the scattering of ultrasonic plane waves on a turbulent jet in air ($Pr = 0.7$). The jet is weakly heated so that the temperature fluctuations act as a passive scalar. In the backscattering geometry one measures the Fourier components of the temperature field $\tilde{T}(q, t)$. The time averaged characteristics are analyzed in detail; in particular we observe a Kolmogorov “ $-5/3$ ” power law behavior for the passive scalar spectrum in the inertial range of scales. The study of the time fluctuations shows that the histograms of $\tilde{T}(q, t)$ remain close to a Gaussian at all scales.

1. Introduction

The mixing of a passive scalar by a turbulent flow is an important problem in a wide variety of situations, both natural (*e.g.* fluid dynamics in the ocean and the atmosphere) and industrial (*e.g.* the homogenization of multi-component fluid mixtures). Its theoretical relevance lies in the fact that the passive “tracer” is advected by the velocity flow field, thus probing the transport properties of turbulence. Considerable efforts — theoretical, numerical and experimental — have been devoted to this problem (see [1] for an introduction). Although the existence of a $k^{-5/3}$ power spectrum for the passive scalar has been the subject of some controversy [2], its existence seems now established [3] experimentally. On the other hand, numerous studies have shown the anomalous scaling behavior of passive scalar increments. Much effort is now devoted to understanding this behavior.

In this work we explore the possibility of using sound scattering as a spectral probe of temperature fluctuations (considered as a passive scalar) in a turbulent flow. Such a non-intrusive measurement probes the scalar field directly in Fourier space and its development can lead to a direct measurement of the dynamics and interactions between scales.

The interaction of a sound waves with a fluid flow has been pioneered by Lighthill and Tatarski and have since then been the subject to continuous developments [1, 4–8]. We adopt

(*) Author for correspondence (e-mail: pinton@physique.ens-lyon.fr)
(**) CNRS URA 1325

here an experimentalist point of view, *i.e.* we consider the use of a wave to probe a medium that interacts with it. Indeed, sound wave propagation is modified by the presence of vorticity and temperature fluctuations, so that sound scattering can be used as a tool of investigation of flow structures. Compact and elegant expression have recently been established by Lund and co-workers for the scattering of sound at low Mach numbers [9–11]. Their findings rely on a first Born approximation and may be summarized as follows: for a plane incoming ultrasonic wave of frequency ν_0 and amplitude P_0^{inc} the scattered pressure at angle θ and distance D in the far field limit, is expressed as:

$$P_{\text{scat}} = P_{\text{scat}}^{\text{vort}} + P_{\text{scat}}^{\text{temp}}, \quad (1)$$

with

$$P_{\text{scat}}^{\text{vort}}(\mathbf{D}, \nu) = P_0^{\text{inc}} \frac{e^{i\nu r/c_0}}{r} \frac{-\cos\theta \sin\theta}{1-\cos\theta} \frac{i\pi^2\nu}{c_0^2} \tilde{\Omega}_{\perp}(\mathbf{q}, \nu - \nu_0), \quad (2)$$

$$P_{\text{scat}}^{\text{temp}}(\mathbf{D}, \nu) = P_0^{\text{inc}} \frac{e^{i\nu r/c_0}}{r} \frac{\pi^2\nu^2}{c_0^2 T_0} \cos\theta \tilde{T}(\mathbf{q}, \nu - \nu_0), \quad (3)$$

where $\mathbf{q} = \mathbf{k}_d - \mathbf{k}_i$ is the scattering wavevector, c_0 the speed of sound at temperature T_0 , $\Omega_{\perp}(\mathbf{r}, t)$ the component of the vorticity field perpendicular to the scattering plane and $T(\mathbf{r}, t)$ the temperature field. We use the notation $\tilde{F}(\mathbf{q}, \nu)$ for the space and time Fourier transform of a field $F(\mathbf{r}, t)$. Note that the scattering due to the vorticity has a quadrupole structure with a main contribution in the forward direction whereas the temperature induced part is of dipole nature and has equal contributions in the forward and backward directions. This difference makes it possible to separate the two effect when both are present.

In the case of isothermal flows, the vorticity contribution is singled out. The validity of equation (2) has been checked experimentally in this case [12,13] using the von Kármán vortex street as a test flow; its use for the study of turbulent flows has also been investigated [14–16].

However, non-isothermal flow are of practical importance (convective flows, heated jets) and hard to study using conventional local probes. Local velocity and/or temperature probes are intrusive and must be adjusted to the particular flow under study. Non-intrusive local velocity measurements can be performed *via* LDV, but only in transparent fluid and its interpretation may be difficult when high temperature gradients develop in the flow. On the other hand, temperature measurements with a short time responses have only been developed using cold wire techniques [17–19], which are intrusive although reliable. We study here the possibility of using sound scattering by temperature inhomogeneities as a tool for performing measurements in a non-isothermal flow. Indeed, using a backscattering geometry it is possible to remove the contribution due to the vorticity field fluctuations. The test flow is a heated jet, at moderate Reynolds numbers.

2. Flow and Measurement Technique

The experimental set-up is sketched in Figure 1a. Air is the working fluid. An open jet is produced with a rotating (dc) fan placed between a simple conical converging inlet (length 30 cm, slope 30 degrees) and a strait cylindrical outlet, 34 cm long and with diameter $D = 10$ cm. The flow speed U is adjustable between 50 and 300 cm/s, so that the Reynolds number $\text{Re} = UD/\mu$ varies in the range 3×10^3 to 4×10^4 (μ is the kinematic viscosity, this unusual notation being chosen to avoid confusion with the temporal frequency ν of Eqs. (2) and (3)).

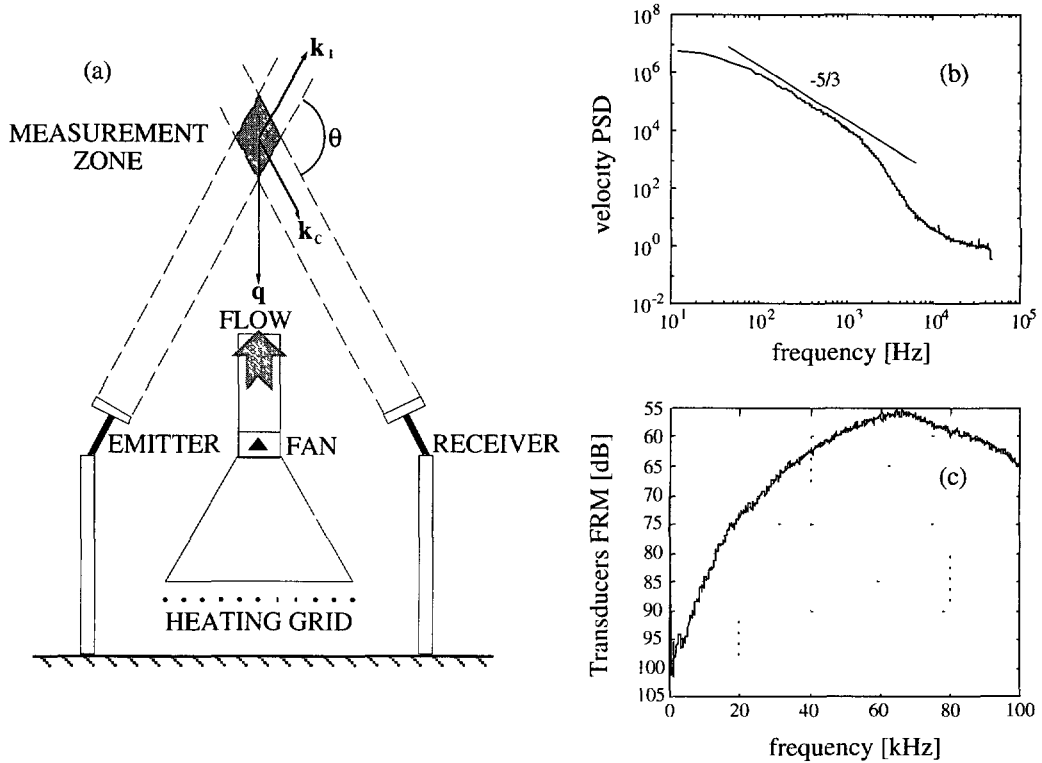


Fig. 1. — (a) Sketch of the experimental set-up. (b) Hot-wire measurement of the kinetic energy spectrum $E(q)$ of velocity fluctuations at $h/D = 3.5$, for $Re = 25\,000$. The straight line corresponds to the Kolmogorov scaling. (c) Frequency response of the emitter-receptor Sell transducers.

A heating grid is positioned upstream of the convergent part. Its power consumption is adjustable, up to 1500 W. The air temperature at the jet nozzle is 15 °C above ambient, and the rms fluctuations in the flow are up to 0.8 degrees, depending upon jet velocities and distance to the nozzle. The ratio of temperature diffusion to advection — measured by the Péclet number $Pe = UL/\kappa$, where κ is diffusivity — is very small ($< 10^{-4}$), and so is the ratio of buoyancy forces to inertia forces ($g\alpha\Delta T/(U^2/L) < 10^{-3}$). In these conditions, comparable to previous experimental studies, the temperature field in the flow is regarded as a passive scalar. We have also checked this on local velocity measurement characteristics with and without heating of the flow.

The local velocity measurements are performed using a calibrated 1 mm long, 10 μm thick hotfilm probe (TSI 1260A-10), connected to a TSI IFA100 anemometer. A typical spectrum of velocity fluctuations is presented in Figure 1b where a Kolmogorov scaling can be observed over one decade of scales (due to the presence of grids at the jet outlet, the turbulence develops rapidly downstream of the jet nozzle).

Local temperature measurements are performed using a Thermometrics 5 μm thick thermistor (model B05PA103N). Its cut-off frequency is about 40 Hz, of the order of the large scale eddy turn-over time ($T \sim D/U_{\text{max}} \sim 30$ Hz). As a result it detects the fluctuations due to the large scale dynamics and thus allows the characterization of the intensity of the rms temperature fluctuations.

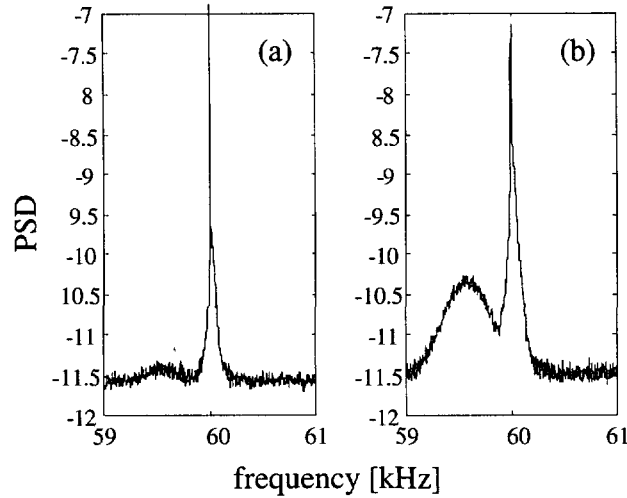


Fig. 2. — Scattering spectra, measured at $h/D = 3.5$, $Re = 7000$ for an incoming sound frequency $\nu_0 = 60$ kHz ($q = 19.2$ cm $^{-1}$), (a) for the isothermal jet and (b) with 0.7 degree of rms temperature fluctuations.

Reversible acoustic transducers (diameter $\Lambda = 8$ cm) of the Sell type [20] are used to generate the incoming sound and to detect the scattered wave. The characteristic velocity of the sound wave is 1 cm/s, much smaller than the typical velocities in the fluid flow. Incident sound frequencies are adjustable in the range $\nu_0 \in [10, 100]$ kHz, corresponding to wavelength $\lambda \in [30, 3]$ mm. The scattered amplitude, measured on the Sell receiver *via* a Bruel & Kjaer 2635 charge amplifier, is recorded on a HP3562 spectrum analyzer. See Figure 1c for the frequency response of the transducers. Most measurements are performed at a fixed scattering angle $\theta = 120$ degrees; in such conditions the scattering wavevector varies in the range 2 to 35 cm $^{-1}$, so that the flow is probed at scales between 2 and 30 mm, corresponding to the inertial range of the turbulent jet flow. Indeed, local velocity measurements yield Taylor microscales in the range [0.7, 2] mm for the explored range of Reynolds numbers. The acoustic transducers are located at distance $D \sim 1$ m, into the far field region ($D_{FF} \sim \Lambda^2/\lambda \sim 0.5$ m at 100 kHz). The spectral resolution increases with the size of the measurement zone: $\delta q \sim 1/L = \cos(\theta/2)/\Lambda$. We thus have here $\Delta q/q \sim c_0 \cos(\theta/2)/\Lambda \nu_0$, varying from 20% down to 3% in the range of explored frequencies. Lastly, we stress that the acoustic Sell transducers are linear so that the phase of the scattered sound is recorded.

3. Results

3.1. TIME-AVERAGED CHARACTERISTICS. — We first describe the time-averaged measurements on the heated jet and show how the spectral nature of the measurements yields a global characterization of the flow.

3.1.1. *Spectral Content of the Detected Acoustic Signal.* — Figure 2a shows the (time) spectrum of the acoustic pressure recorded by the transducer, in the back-scattering geometry and in the case of an isothermal jet. One observes a single spectral line at the frequency of the incoming sound; this line (hereafter called the reference peak), equally present when flow is stopped, is due to the echos of the incoming sound wave across the measurement room.

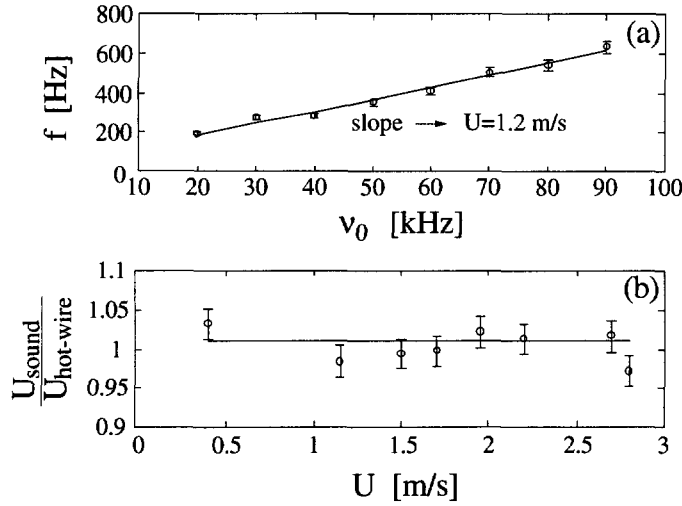


Fig. 3. — Measurement at $h/D = 3.5$, for $T_{\text{rms}} \sim 1$ °C. (a) Variation of the Doppler shift with the incoming sound frequency; the slope $|df/d\nu_0| = 2 \sin(\theta/2)U/c$ yields the average jet speed in the measurement zone. (b) Ratio of jet speeds measured from the Doppler shift and from hot wire anemometry (the local probe being placed at the center of the acoustic measurement volume).

As the heating is turned on, so that temperature fluctuations are present in the flow, one observes a spectrum like the one shown in Figure 2b. In addition to the reference peak a band of excited frequencies appears. It corresponds to the scattering of the incoming sound wave by the temperature inhomogeneities in the flow. The maximum is Doppler shifted from the reference peak because of the mean advection velocity in the jet. Indeed, if ν_0 is the frequency of the incident wave with wavevector \mathbf{k}_i , the fluid particles moving with velocity \mathbf{u} in the jet see an incoming sound frequency equal to $\nu_1 = \nu_0 - \mathbf{k}_i \cdot \mathbf{u}/2\pi$ and scatter a wave with identical frequency in their own reference frame (at low Mach numbers the scattering is considered elastic). The scattered wave in the direction \mathbf{k}_d is then observed with a frequency $\nu_1 + \mathbf{k}_d \cdot \mathbf{u}/2\pi$ by a transducer fixed in the laboratory reference frame. The net Doppler shift is thus $f = (\mathbf{k}_d - \mathbf{k}_i) \cdot \mathbf{u}/2\pi = \mathbf{q} \cdot \mathbf{u}/2\pi$, where \mathbf{q} is the scattering wavevector.

In the next section, we discuss the time-averaged characteristics of this Doppler shift.

3.1.2. Doppler Shift: Position. — Let us perform a Reynolds decomposition of the velocity field, so that the velocity of a fluid particle is expressed as: $\mathbf{u} = \mathbf{U} + \mathbf{u}'$ where \mathbf{U} is the average jet speed and \mathbf{u}' represents the turbulent fluctuations (here $u'_{\text{rms}}/U \sim 25\%$ as customary in open jets). Then the scattered sound has a maximal spectral component at frequency $\nu = \nu_0 + f = \nu_0 + \mathbf{q} \cdot \mathbf{U}/2\pi$, the measurement of which gives access to the mean velocity in the flow. In our symmetrical experimental set-up, \mathbf{q} and \mathbf{U} are anti-parallel, and one has:

$$U = \frac{-f c_0}{2\nu_0 \sin \frac{\theta}{2}}. \quad (4)$$

This is well-confirmed by our experimental observations: Figure 3a illustrates the linearity of the Doppler shift when the incoming sound frequency is varied and Figure 3b compares the mean velocity derived from the slope of plots such as 3a with direct measurements using local hot-wire anemometry in the center of the scattering volume.

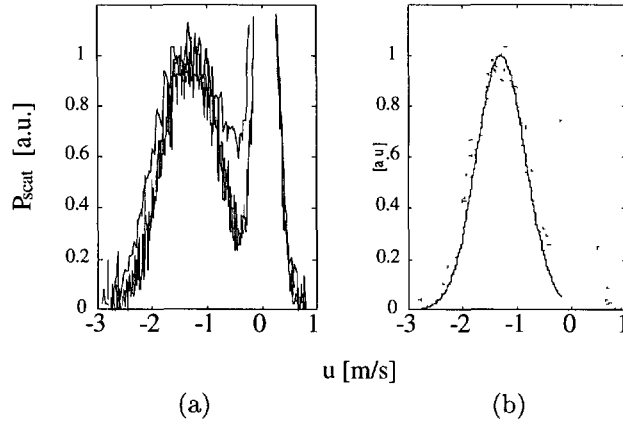


Fig. 4. — (a) Scattering spectra for $\nu_0 = 20$ kHz ($q = 6.4 \text{ cm}^{-1}$) and $\nu_0 = 90$ kHz ($q = 28.9 \text{ cm}^{-1}$). Measurements made at $h/D = 3.5$; the x -axis is rescaled from frequency to velocity units, using the Doppler shift relation $u = 2\pi f/q$. (b) Scattering spectrum at $\nu_0 = 90$ kHz, compared to a histogram of velocity measurement using hot-wire anemometry, at $h/D = 3.5$.

This very good agreement with the local measurements validates a possible use of acoustic scattering as a remote sensing technique for average velocity measurements in non-isothermal flows. Indeed in many instances (*e.g.* factory chimneys or jet engines) these flows cannot be conveniently probed with local sensors. Hot-wire measurements are sensitive to chemical contamination of the sensing element and need constant compensation for temperature fluctuations [21,22]; Laser Doppler Anemometry requires a high degree of precision in the geometrical alignment of the laser beams and is quite expensive, as other radio-acoustic techniques [23,24]. We note that acoustic velocimetry devices operating on principles similar to that of radars (measurement of time-lags and Doppler shifts of echos) have been developed (and are commercial) for measurements in liquids [25,26]; however they require seeding of the flow.

3.1.3. Doppler Shift: Broadening. — The broadening of the Doppler frequency line — $2\pi\delta f = (\delta\mathbf{q}) \cdot \mathbf{U} + \mathbf{q} \cdot (\mathbf{u}')$ — has two sources: one is due to diffraction, *i.e.* to the finite size L of the measurement volume ($\delta q \sim 2\pi/L$); the other is due to the velocity fluctuations \mathbf{u}' in the jet. The relative importance of the two terms depends on the frequency of the incoming wave:

$$\frac{\delta f_{\text{diffraction}}}{\delta f_{\text{advection}}} \sim \frac{\delta\mathbf{q} \cdot \mathbf{U}}{\mathbf{q} \cdot \mathbf{u}'} \sim \frac{\lambda/L}{u'/U}, \quad (5)$$

where λ is the sound wavelength.

Figure 4a shows superimposed scattering spectra for increasing ν_0 ; the x -axis as been rescaled in units of velocity, using the Doppler relation. As can be observed the width of the Doppler hump decreases for increasing sound frequencies because the diffraction effect is reduced. In the limit of high frequencies, the Doppler broadening is only due to the velocity fluctuations in the jet, $\delta f/f \sim u'/U \sim 25\%$, as can be observed in Figure 4b where a histogram of velocity fluctuations (recorded from conventional hot-wire anemometry) is superimposed to a scattering spectrum at high ν_0 . The two curves almost collapse, since in this case $\delta f_{\text{diffraction}}/\delta f_{\text{advection}} < 5\%$. Comparing again with Figure 4a, it is observed that for almost all sound frequencies the advection term is dominant in the broadening of the Doppler peak.

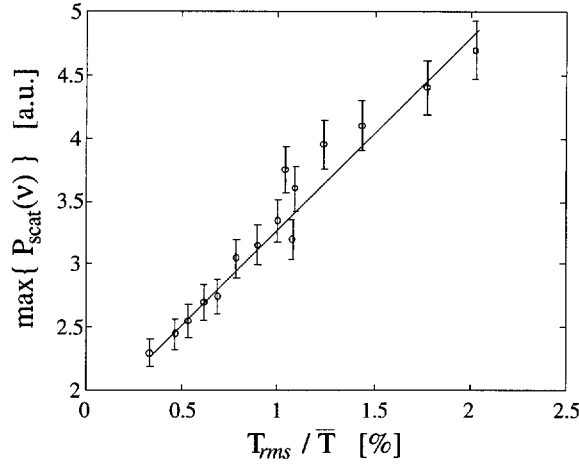


Fig. 5. — Variation of the amplitude of scattered sound, defined as the maximum of the Doppler peak, with the amplitude of temperature fluctuations. Measurement at $h/D = 3.5$, $Re = 7000$ and for $q = 19.2 \text{ cm}^{-1}$

3.1.4. Amplitude of the Scattered Pressure: Linearity with T_{rms}/\bar{T} . — We now consider the amplitude of the scattered sound and we first study its variation with the intensity of the temperature fluctuations in the flow. To wit, we operate in a given flow configuration ($h/D = 3.5$, $Re = 7000$) and for a fixed scattering wavenumber $q = 19.2 \text{ cm}^{-1}$ (corresponding to a length scale of 3 mm, well inside the inertial range). We then measure the amplitude of the scattered sound defined as the maximum of the Doppler peak. Results are shown in Figure 5. The temperature fluctuations $t' = T_{rms}/\bar{T}$ are independently measured locally at the center of the scattering volume using the $5 \mu\text{m}$ thermistor. The linearity is in agreement with equation (3). Note that, as an alternative possibility for the definition of the scattered sound amplitude, we could integrate $P_{scat}(\nu)$ over the width of the Doppler peak. This again yields a linear behavior of P_{scat} vs. t' since the Doppler peak has a Gaussian shape following that of the velocity fluctuations, if one neglects diffraction.

3.1.5. Amplitude of the Scattered Pressure: Spectrum $\tilde{T}(q)$. — We then consider the spatial spectrum of the variance of the temperature (passive scalar) fluctuations in the flow. For this purpose, we record the sound amplitude as the scattering wavenumber is varied. We operate at fixed $\theta = 120$ degrees, and vary the incoming sound frequency between 10 and 100 kHz. For each frequency, we measure the amplitude of scattered peak. We then use the calibration curve of the transducers to deduce the scalar spectrum $E_\theta(q)$ — defined such that $E_\theta = \bar{T}^2 = \int E_\theta(q) dq$. The results are reported in Figure 6a for two values of the Reynolds number $Re = 7000$, corresponding to $R_\lambda \sim 60$, and $Re = 25000$, corresponding to $R_\lambda \sim 230$.

In each case one observes a $k^{-5/3}$ scaling region, as predicted by Obukhov [27] and Corrsin [28]. Indeed in air the Prandtl number is close to one and the Corrsin–Obukhov length scale η_{CO} is almost equal to the Kolmogorov dissipation length η , so that the passive scalar spectrum is dominated by advection effects. Accordingly, we also observe in Figure 6a that the high wavenumber cut-off increases with the Reynolds number.

To show that the scaling region occurs in the inertial range as defined by velocity measurements, we have plotted in Figure 6b the kinetic energy spectra recorded by a local probe located at the center of the acoustic measurement volume, in the same flow conditions as Figure 6a.

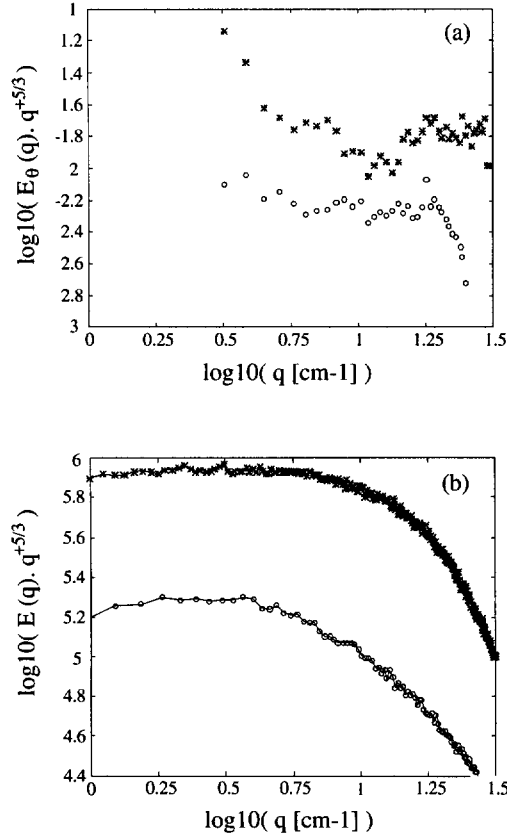


Fig. 6. — (a) Variance spectrum of temperature fluctuations $E_\theta(q)$ from acoustic scattering measurement; $h/D = 3.5$, (*): $Re = 7000$, (o): $Re = 25000$. (b) corresponding kinetic energy spectrum $E(q)$ from hot-wire anemometry at the center of the scattering volume (the axis being rescaled in units of wavenumbers using the Taylor hypothesis).

We observe that although the scaling domains are similar, some differences are worth noting:

- (i) the acoustic measurement is limited at low frequency by the size of the transducers, so it is not easy to check if the scaling domain for $E_\theta(q)$ extends towards low wavenumbers as it does for $E(q)$;
- (ii) the scaling domain for $E_\theta(q)$ seems to extend somewhat further toward the high wavenumber side and with a steeper cut-off than the velocity spectrum. This last effect has already been observed in acoustic measurement of the vorticity spectrum $E_\omega(q)$ [14]. It is thus not clear if this is an effect of the measurement method or an intrinsic feature of the passive scalar spectrum, whose cut-off region is still the subject of many controversies [30].

3.2. TEMPORAL DYNAMICS. — We now analyze the temporal dynamics of the Fourier components of the temperature fluctuations $\tilde{T}(q, t)$. Figure 7a shows a contour plot of a short-time Fourier analysis of the pressure signal on the receiver, for $Re = 7000$, and q in the inertial range. Besides the always present reference peak, one observes that the scattered Doppler peak

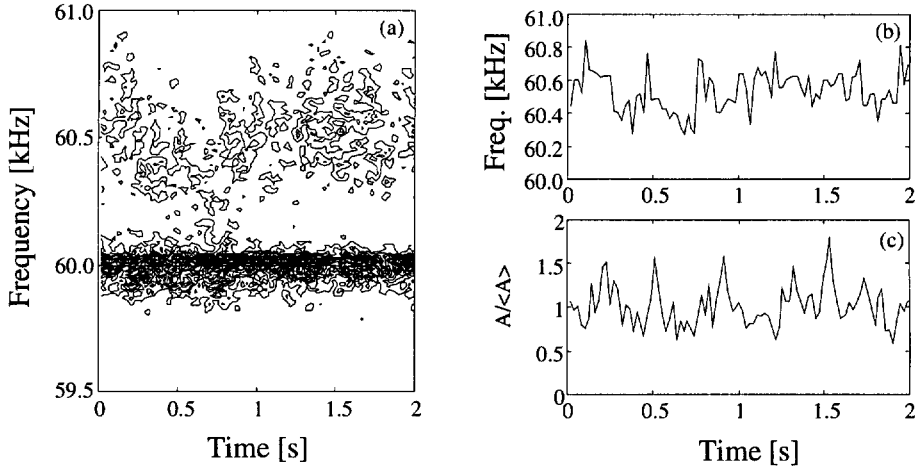


Fig. 7. — (a) Contour plot of a short time Fourier analysis of the acoustic pressure, $Re = 7000$, $h/D = 3.5$, $q = 19.2 \text{ cm}^{-1}$; for the same time period: variation of the frequency at which the maximum of the scattered peak is observed (b) — Doppler shift — and of the maximum amplitude (c), scaled with its average value.

fluctuates noticeably, both in position and amplitude. Indeed, Figure 7b shows the corresponding time fluctuations of the position of the maximum of the scattered peak (Doppler shift): one observes the characteristic high level of average velocity fluctuations in a jet (about 25%). In the same manner, Figure 7c shows for the same time period the fluctuations of the amplitude of the Doppler peak, normalized by its mean value. Again one observes large and rapid fluctuations, which we now describe in greater details.

The scattered contribution to the acoustic pressure $P_{\text{scat}}(q, t)$ is obtained from a band-pass filtering of the pressure signal on the receiver, in order to eliminate the reference peak. The width of the band-pass filter (we use a 7-pole Butterworth scheme) is chosen to cover all possible Doppler shifts of the scattering sound. In the backscattering geometry, we then have: $P_{\text{scat}}|_{\text{filtered}} \propto \tilde{T}(\mathbf{q}, t)$. The resulting time series is shown in Figure 8, where we have plotted $\tilde{T}(\mathbf{q}, t)$ normalized by its rms intensity (the natural scale since the mean value is zero). It can be observed that it displays large fluctuations in time, although it is a spatially averaged quantity. We note that such non-trivial temporal fluctuations has already been observed for other global quantities such as the pressure or the power consumption of a turbulent flow [31, 32].

From the time evolution we now compute the Probability Density Functions (PDFs) of $\tilde{T}(q, t)$ for varying wavenumbers q — see Figure 9. It is readily observed that they are almost (but not quite) Gaussian for all wavenumbers under analysis. The departure from a Gaussian behavior is systematic with a tendency to form high temperature concentrations at all scales — see Figure 9a. In addition, this behavior seems to increase as smaller scales are investigated as can be observed in Figure 9b where the PDFs for $q_1 = 6.4$ and $q_2 = 31.4 \text{ cm}^{-1}$ are compared. For the corresponding Reynolds number ($R_\lambda = 64$), if one refers to the velocity spectrum, it is found that q_1 lies at the beginning of the inertial range while q_2 is in the dissipative region.

We have also computed the third (skewness), fourth (flatness) and fifth moments of the PDFs, for all scattering wavenumbers. They all tend to increase with increasing wavenumber, *i.e.* decreasing length scale as shown in Figure 10. We emphasize that these changes with scale are much smaller than the corresponding changes in the PDFs of temperature increments as obtained from local analysis, either in experimental measurements [33–35] or in numerical

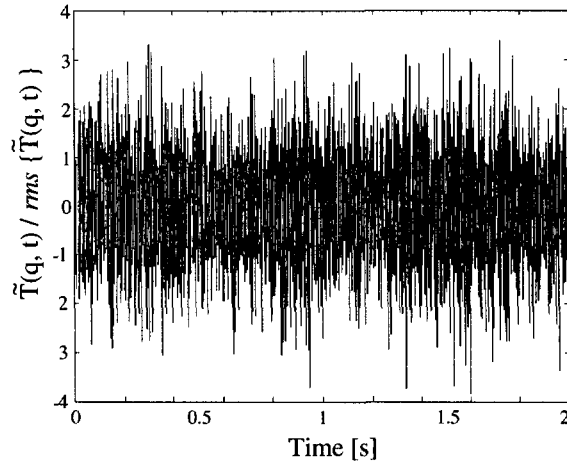


Fig. 8. — $\tilde{T}(q, t)$, scaled by its rms value, as obtained from band-pass filtering of the Doppler peak in the scattered sound. $Re = 7000$, $h/D = 3.5$, $q = 19.2 \text{ cm}^{-1}$

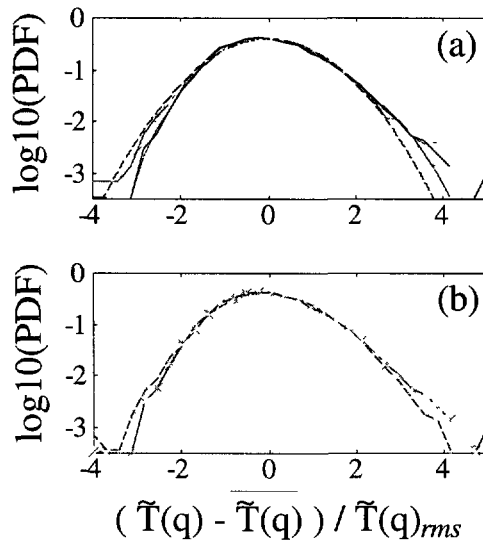


Fig. 9. — PDFs of the time fluctuations of the Fourier components of the temperature field; $Re = 7000$, $h/D = 3.5$. The histograms are calculated for the centered processes, *i.e.* with zero mean and normalized by its variance. (a) $q = 6.4, 9.6, 12.8, 16.0, 19.2, 25.6, 31.4 \text{ cm}^{-1}$; (b) $q = 6.4$ and 31.4 cm^{-1}

simulations [36]. In this respect, there is a net trend to reduction of the intermittency in the spectral measurement of the temperature (passive scalar) field. This result is in agreement with very recent numerical simulations in a flow with a mean temperature gradient [37].

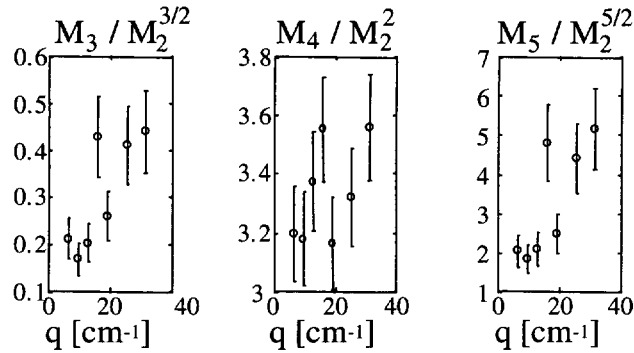


Fig. 10. — Third, fourth and fifth, moments of $\tilde{T}(q, t)$, $\text{Re} = 7000$, $h/D = 3.5$, for $q = 6.4, 9.6, 12.8, 16.0, 19.2, 25.6, 31.4 \text{ cm}^{-1}$

4. Conclusions

The aim of our study was to validate the use acoustic scattering as a spectral non-intrusive measurement of temperature fluctuations in a turbulent flow. We believe that the results of the time averaged characteristics reported in Section 3.1 achieve this goal. The Doppler properties of the the detected acoustic signal are in agreement with a scattering mechanism; band pass filtering allows the separation of the scattered sound from spurious echos and measurement noise. We have also established the linearity of the scattering with the amplitude of the temperature fluctuations and the spectral nature of the measurement. As the wavenumber is varied we have directly measured the spectrum $E_\theta(q)$ which displays a $-5/3$ scaling behavior in the inertial range, as expected in a fluid with Prandtl number of order unity.

We also report preliminary results on the temporal dynamics of the Fourier components of the temperature field. We observe that the PDFs of $\tilde{T}(q, t)$ have very similar shapes, close to a Gaussian, as the wavenumber grows. This behavior is in agreement with recent numerical simulations, but it is in constrast with the behavior of the temperature increments measured with a local probe. Further measurements are needed to investigate in greater details the dynamics of the Fourier components of the scalar field, in particular the simultaneous measurement of several components $\tilde{T}(q_1, t)$, $\tilde{T}(q_2, t)$ etc. This type of multispectral analysis has been performed on measurements of density fluctuations by light scattering [38] and on measurements of vorticity fluctuations using ultrasound scattering [39]. It is currently underway on temperature fluctuations (as a passive scalar).

Acknowledgments

We would like to thank Nicolas Garnier and Christophe Mondies for their participation to some of the measurements reported here, as part of their graduate summer project. We acknowledge useful discussions with C. Baudet and A. Pumir. This work is supported by DRET contract Number 952593A000.

References

- [1] Monin A.S. and Yaglom A.M., *Statistical Fluid Mechanics* (MIT Press, 1971).
- [2] Sreenivasan K., *Proc. Roy. Soc. London* **A434** (1991) 165.
- [3] Jayesh, Tong C. and Warhaft Z., *Phys. Fluids* **6** (1994) 306.
- [4] Obukhov A.M., *Dokl. Akad. Nauk. SSSR* **30** (1941) 611.
- [5] Lighthill M.J., *Proc. Roy. Soc.* **A2111** (1953) 564–587.
- [6] Kraichnan R.H., *J. Acoust. Soc. Am.* **25** (1953) 1096–1109.
- [7] Chernov L.A., *Wave propagation in a random medium* (McGraw-Hill, 1960).
- [8] Tatarskiĭ V.I., *Wave propagation in a turbulent medium* (Dover, 1961).
- [9] Lund F. and Rojas C., *Physica D* **37** (1989) 508–514.
- [10] Contreras H. and Lund F., *Phys. Lett. A* **149** (1990) 127–130.
- [11] Lund F., in *Non linear phenomena in fluids, solids and other complex systems*, P. Cordero and B. Nachtergaele, Eds. (North Holland, 1991).
- [12] Baudet C., Ciliberto S. and Pinton J.F., *Phys. Rev. Lett.* **67** (1991) 193–195.
- [13] Pinton J.F. and Baudet C., in *Turbulence in spatially extended systems*, Les Houches Series, C. Basdevant, R. Benzi and S. Ciliberto, Eds. (Nova Science Publishers, 1993).
- [14] Baudet C. and Hernandez R., in *Advances in Turbulence*, S. Gavrilakis, L. Machiels and P.A. Monkewitz, Eds. (Kluwer, 1996) pp. 421–424.
- [15] Pinton J.-F., Derroncourt B. and Fauve S., in *Advances in Turbulence*, S. Gavrilakis, L. Machiels and P.A. Monkewitz, Eds. (Kluwer, 1996) pp. 437–440.
- [16] Derroncourt B., Pinton J.-F. and Fauve S., submitted to *Physica D*.
- [17] Wyngaard J.C., *Phys. Fluids* **14** (1971) 2052–2056.
- [18] Antonia R.A., Browne L.W.B. and Chambers A.J., *Rev. Sci. Instrum.* **52** (1981) 1382–1385.
- [19] Talby R., Anselmet F. and Fulachier L., *Exp. Fluids* **9** (1990) 115–118.
- [20] Anke D., *Acustica* **30** (1974) 30.
- [21] Corrsin S., *NACA Rep.* **TN1864** (1949).
- [22] Arya S.P.S. and Plate E.J., *Inst. Control Syst.* (1969) 87–90.
- [23] Peters G. and Kirtzel H.J., *Ann. Geophys. Atm. Hydro. and Space Sci.* **12** (1994) 506–517.
- [24] Weber B.L., Wuertz D.B. and Welsh D.C., *J. Atm. Ocean. Tech.* **10** (1993) 452–464.
- [25] Proni J.R. and Apel J.R., *J. Geophys. Rech.* **80** (1975) 1147–1151.
- [26] Lhermitte R., *J. Geophys. Rech.* **88** (1983) 725–742.
- [27] Obukhov A.M., *Izv. Akad. Nauk. SSSR, Geogr. i Geofiz.* **13** (1949) 58–69.
- [28] Corrsin S., *J. Appl. Phys.* **22** (1951) 469–473.
- [29] Batchelor G.K., Howells I.D. and Townsend A.A., *J. Fluid Mech.* **5** (1959) 134–139.
- [30] Kerr R.M., *J. Fluid Mech* **211** (1990) 309–332.
- [31] Fauve S., Laroche C. and Castaing B., *J. Phys. II France* **3** (1993) 271.
- [32] Labbé R., Pinton J.-F. and Fauve S., *J. Phys. II France* **6** (1996) 1099–1110.
- [33] Anselmet F., Gagne Y., Hopfinger E. and Antonia R., *J. Fluid Mech.* **140** (1984) 163.
- [34] Jayesh, Warhaft Z., *Phys. Rev. Lett.* **67** (1991) 3503.
- [35] Marchand M., Thèse de Doctorat, Institut Polytechnique de Grenoble (1992).
- [36] Pumir A., *Phys. Fluids* **6** (1994) 2118 and *Phys. Fluids* **6** (1994) 3974.
- [37] Pumir A. and Brun C., DEA Graduate Report, Université de Nice (1996).
- [38] Grésillon D. and Mohamed-Benkadda M.S., *Phys. Fluids* April (1988).
- [39] Friedt J.-M., Master Report with Baudet C., École Normale Supérieure de Lyon (1996).